JFM RAPIDS
journals.cambridge.org/rapids

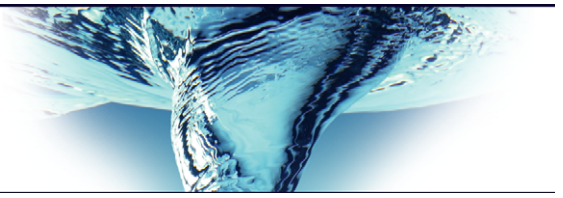

Effect of vortex line distribution in superfluid plane Poiseuille flow instability

R. Sooraj and A. Sameen†

Department of Aerospace Engineering, Indian Institute of Technology Madras, Chennai 600036, India

(Received 5 September 2012; revised 27 November 2012; accepted 11 January 2013; first published online 27 February 2013)

The hydrodynamic stability of plane Poiseuille flow of superfluid is studied using modal and non-modal analysis. Two modes of instability are predicted, in normal mode stability analysis of the normal fluid, one caused by viscosity similar to the classical mode and another due to mutual friction between superfluid and normal fluid. The mutual friction mode occurs at high wavenumbers, which are stable wavenumbers in classical plane Poiseuille flow. A high superfluid vortex line density alone is not enough to induce instability in normal fluid; a localization of vortex lines is shown to play a major role. The extent of vortex line concentration required to cause instability depends on the density itself. Non-modal instability analysis shows that oblique waves are stronger than streamwise waves, unlike the scenario in classical plane Poiseuille flow.

Key words: complex fluids, instability, quantum fluids

1. Introduction

The hydrodynamics of superfluid flow is best explained by Landau's two-fluid model, and it has given interesting insights into the classical and quantum behaviour of the system, see for example, Landau & Lifshitz (1959), Vinen & Niemela (2002) and Tilley & Tilley (2005). This model considers He-II as an intimate mixture of two fluid components, a viscous normal fluid and an inviscid superfluid, with different velocity fields ($\boldsymbol{V}_n$ and $\boldsymbol{V}_s$) and densities (ρ_n and ρ_s). Superfluid flow is dissipationless if the relative velocity is below some critical value (Tough 1982), above which there is dissipation associated with triggering of turbulence in the superfluid. Because of the existence of two velocities, turbulence in He-II can be co-flow turbulence or counterflow turbulence, based on whether the two components are moving in the same direction or in opposite directions. Co-flow turbulence is analogous to classical turbulence, whereas counterflow turbulence is excited by thermal counterflow

† Email address for correspondence: sameen@ae.iitm.ac.in

 © Cambridge University Press 2013
doi:10.1017/jfm.2013.35

https://doi.org/10.1017/jfm.2013.35 Published online by Cambridge University Press

(Barenghi 2001). The turbulence in superfluid consists of a tangle of quantized vortex lines which scatter the normal fluid leading to a dissipative interaction between the two fluids, called the mutual friction (Vinen 1957). The mechanism triggering turbulence is not clearly known in either co-flow or counter-flow scenarios (Haas *et al.* 1974; da Haas & van Beelen 1976). Analysing the various experimental results, Tough (1982) pointed out that two different states of counterflow turbulence exist, the T1 and T2 states, marked by sudden jumps in superfluid vortex line densities. He argued that in the T1 state only superfluid becomes turbulent whereas in the T2 state both the superfluid and normal fluid become turbulent. Linear modal stability analysis of normal fluid in thermal counterflow through a circular pipe reveals that the transition from T1 to T2 is an instability of normal fluid due to the action of superfluid vortices (Melotte & Barenghi 1998). In this paper, however, we study instability in co-flow of He-II in plane channel flow.

Co-flow turbulence is more interesting because of its similarities with classical turbulence (Vinen 2006). Most studies in co-flow turbulence in He-II were focused on measuring the velocity spectrum and comparing it with that of classical fluids, see a recent review by Skrbek & Sreenivasan (2012). However, studies on the transition of laminar to turbulent flow in co-flow of He-II have rarely been reported. Donnelly & Lamar (1988) experimentally investigated the stability characteristics of flow of He-II between rotating concentric cylinders and showed that the nucleation of quantized vortices alters its characteristics from those of classical fluids. Barenghi & Jones (1988) confirmed Donnelly & Lamar (1988)'s arguments with a numerical study on the stability characteristics and showed the effect of vortex tension in altering the stability. Godfrey, Samuels & Barenghi (2001) studied co-flow of He-II using a linear modal stability analysis in a channel using the two-fluid model. They showed that two modes of instability are possible, one similar to classical fluids and the other a low-wavenumber instability. The action of superfluid vortices did change the velocity profile, but was considered to be independent of Reynolds number, Re, as also reported in Sooraj & Sameen (2011), which need not be true. Bergström (2008) studied the transient growth of three-dimensional disturbances in plane Poiseuille flow of He-II using non-modal analysis. A substantial increase in transient growth of three-dimensional perturbations, in comparison with classical fluids, was observed in normal fluid due to the action of mutual friction from the superfluid. Mutual friction was shown to affect the transient growth characteristics in two ways: by reducing the damping of disturbances and by altering the mean flow. The present work shows the effect of vortex line density distribution in determining the stability of normal flow using a modal and non-modal analysis and is different from previous stability studies in two aspects. First, because of the absence of a base-flow similarity relation, an appropriate velocity profile is computed for every Reynolds number. Secondly the sign of the mutual friction term in the governing equation is different as discussed below and in Sooraj & Sameen (2011).

The system is governed by two separate equations for momentum conservation of the two fluids, which are coupled through the mutual friction force. The equations for the normal fluid are considered here, keeping the effect of the superfluid fixed through mutual friction. The momentum conservation for the normal fluid, in the absence of temperature gradient, in non-dimensional form is written as (Tough 1982; Melotte & Barenghi 1998)

$$\frac{\partial}{\partial t}\boldsymbol{V}_n + (\boldsymbol{V}_n \cdot \nabla)\boldsymbol{V}_n = -\nabla P + \frac{1}{Re}\nabla^2 \boldsymbol{V}_n - \boldsymbol{F}_{mf}, \tag{1.1}$$

https://doi.org/10.1017/jfm.2013.35 Published online by Cambridge University Press

where P is pressure and Re is the normal-fluid Reynolds number defined with the viscosity ν_n of the normal fluid; suffix n denotes normal fluid throughout this paper. The centreline velocity of the normal fluid, V_0, and channel half-width, L, are the velocity and length scales used for non-dimensionalizing. $\boldsymbol{F}_{mf}$ is the dissipative mutual friction interaction between the two fluid components, defined as (Donnelly & Swanson 1986)

$$\boldsymbol{F}_{mf} = \left(\frac{B\rho_s L\kappa}{2\rho V_0}\right)\frac{2}{3}l(\boldsymbol{V}_n - \boldsymbol{V}_s), \tag{1.2}$$

where B is the mutual friction coefficient, $\kappa = h/m_4$ is the quantized circulation, where h is Planck's constant and m_4 is the mass of an ^{4}He atom, and l is the superfluid vortex line density i.e. total length of quantized superfluid vortex lines per unit volume; subscript s denotes superfluid. The mutual friction term in the governing equations in Godfrey *et al.* (2001) and Bergström (2008) posses a sign different from that in Tough (1982). In this work the sign as in Tough (1982) and Tilley & Tilley (2005) is followed, because mutual friction will decelerate the normal fluid as reported in Hall & Vinen (1956*a*,*b*), which is more appropriate as also discussed in Sooraj & Sameen (2011). The above mutual friction can be simplified as (Godfrey *et al.* 2001)

$$\boldsymbol{F}_{mf} = f(z)(\boldsymbol{V}_n - \boldsymbol{V}_s). \tag{1.3}$$

The function $f(z)$ gives the distribution of superfluid vortex lines along the wall-normal direction z. Comparing (1.2) and (1.3), assuming B and κ are constants for given temperature, the dependence of $f(z)$ on z comes from l which is the vortex line density. Numerical simulations by Samuels (1992) and Aarts & de Waele (1994) based on vortex dynamics show that the superfluid vortex lines tend to move towards points where superfluid and normal-fluid velocities are equal. Therefore a bimodal Gaussian distribution is assumed for the superfluid vortex line distribution, having the peaks at points of zero relative velocity between the two fluids. The assumed distribution with standard deviation σ is written as (Godfrey *et al.* 2001; Bergström 2008)

$$f(z) = f_{max}\{\exp[-(z - z_-)^2/2\sigma^2] + \exp[-(z - z_+)^2/2\sigma^2]\}, \tag{1.4}$$

where $z_\pm$ are the points of zero relative velocity and f_{max} is the maximum value of $f(z)$. A sample $f(z)$ distribution is given in figure 1. As (1.4) suggests, an increase in σ means an increase in uniformity of the vortex line distribution. The strength of the mutual friction term is characterized by parameter f_{max}. A given combination of σ and f_{max} depicts a situation of superfluid flow at some particular temperature (Bergström 2008).

2. Base flow

The classical parabolic velocity profile for plane Poiseuille flow is modified due to mutual friction. This modified profile is numerically calculated from the momentum equation for the normal fluid with a steady and parallel flow assumption and no-slip boundary condition at the walls. Equation (1.1) takes the form

$$-\frac{\mathrm{d}P}{\mathrm{d}x} + \frac{1}{Re}\frac{\mathrm{d}^2U_n}{\mathrm{d}z^2} - f(z)[U_n - U_s] = 0. \tag{2.1}$$

$U_n(z)$ and U_s are the normal-fluid and superfluid velocities along streamwise direction. The pressure gradient is chosen such that $Re\,\mathrm{d}P/\mathrm{d}x = -2$, as in the case of classical

https://doi.org/10.1017/jfm.2013.35 Published online by Cambridge University Press

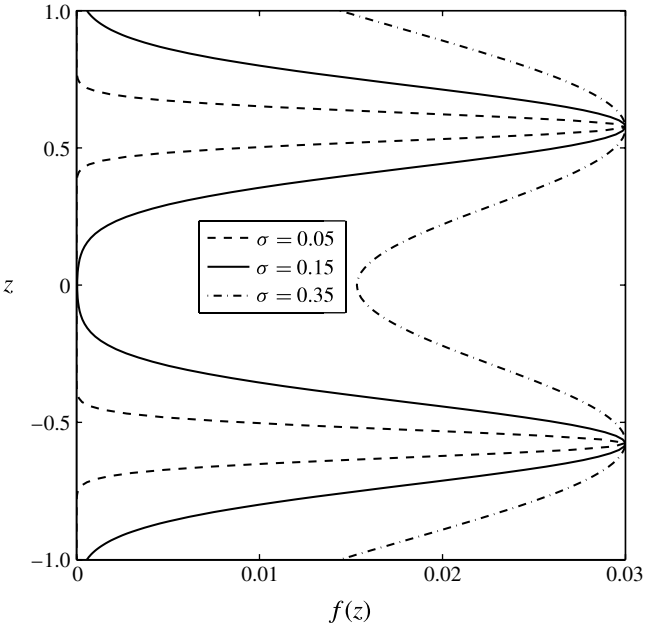

FIGURE 1. Superfluid vortex line distribution $f(z)$ along the wall-normal direction. $f_{max} = 0.03$ for all cases shown.

fluid (Barenghi, Donnelly & Vinen 1983; Donnelly 1991; Bergström 2008). Since U_s is assumed inviscid, the superfluid velocity is constant across the channel width. (In co-flowing He-II in isothermal conditions the average velocities of the two components are equal, i.e. $\int_{-1}^{1} U_n \, \mathrm{d}z = \int_{-1}^{1} U_s \, \mathrm{d}z = 2U_s$ which implies $U_s = 2/3$. It can be easily shown that the volume flow rates of both the components are equal (Godfrey *et al.* 2001).) It is clear that, unlike classical fluids, the mean flow profile calculated from the non-dimensional equation is not self-similar with respect to the normal-fluid Reynolds number as shown figure 2. The deviation of the normal flow profile from classical plane Poiseuille flow increases with Reynolds number and the profile becomes more flattened as Reynolds number increases. A recent experiment by Guo *et al.* (2010) using the molecular tagging method visualized the velocity profile for a counter-flowing normal fluid. They observed the normal fluid to have flat velocity profile for heat fluxes well above a critical value required for the onset of quantum turbulence. In view of the high broadening rates of molecule lines, they attribute the flattening of the profile to turbulence in the normal fluid rather than due to mutual friction. However further experiments are required to make it clear whether the state is 'laminar, turbulent or doubly turbulent?' as Barenghi (2010) suggests in a review on this work. Guo *et al.* (2010) in their conclusion point to a possibility of both superfluid and normal fluid becoming turbulent and velocity profiles being flattened. The flattening of the normal-fluid profile may be achieved in (2.1) at high f_{max} or σ. It is to be recalled that the present stability analysis is for a co-flowing superfluid.

https://doi.org/10.1017/jfm.2013.35 Published online by Cambridge University Press

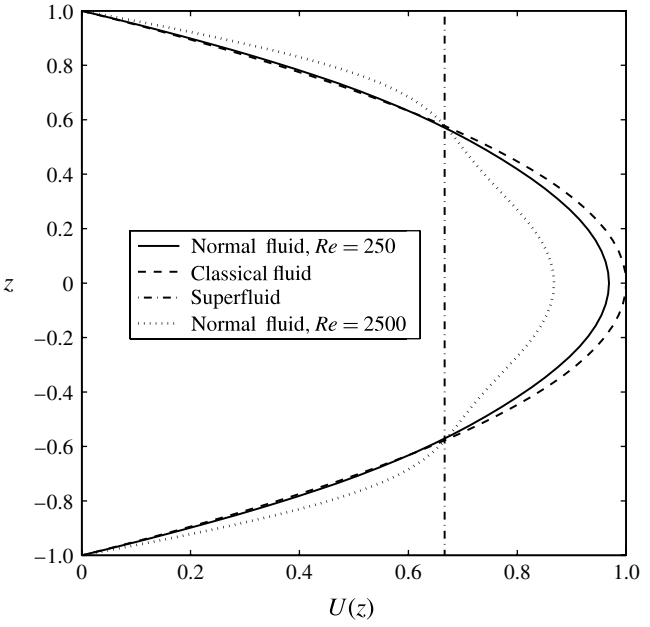

FIGURE 2. Sample velocity profiles of normal fluid, superfluid, and classical fluid. Velocity profile for normal fluid calculated with $f_{max} = 0.03$ and $\sigma = 0.15$.

3. Stability of the normal fluid

Stability of the normal fluid is studied by perturbing the normal fluid while keeping the superfluid part unperturbed. We are interested in the temporal stability of the normal fluid where the nature of the time evolution of the perturbations is studied. The standard procedure in Schmid & Henningson (2001) is followed to derive the linearized perturbation equations from the normal-fluid momentum equation, which forms an eigenvalue problem. The modified Orr–Sommerfeld and Squire's equations for the perturbation velocity, v_n, and vorticity, η_n, in the normal direction are written in matrix form as

$$-\mathrm{i}\omega \begin{pmatrix} k^2 - \mathrm{D}^2 & 0 \\ 0 & 1 \end{pmatrix} \begin{pmatrix} \tilde{v}_n \\ \tilde{\eta}_n \end{pmatrix} + \begin{pmatrix} L_{OS} & 0 \\ \mathrm{i}\beta U_n{}' & L_{SQ} \end{pmatrix} \begin{pmatrix} \tilde{v}_n \\ \tilde{\eta}_n \end{pmatrix} = 0, \tag{3.1}$$

where

$$L_{OS} = \mathrm{i}\alpha U_n(k^2 - \mathrm{D}^2) + \mathrm{i}\alpha U_n{}'' + \frac{1}{Re}(k^2 - \mathrm{D}^2)^2 - [f'(z)\mathrm{D} + f(z)\mathrm{D}^2 - k^2 f(z)], \tag{3.2}$$

$$L_{SQ} = \mathrm{i}\alpha U_n + \frac{1}{Re}(k^2 - \mathrm{D}^2) + f(z). \tag{3.3}$$

A prime on a quantity indicates the derivative in the z-direction of that quantity, D represents the differential operator in the z-direction ($\partial/\partial z$) and k is defined such that $k^2 = \alpha^2 + \beta^2$ where α and β are the wavenumbers of perturbations in the streamwise direction x and spanwise direction y respectively. The matrix equation (3.1) is solved

https://doi.org/10.1017/jfm.2013.35 Published online by Cambridge University Press

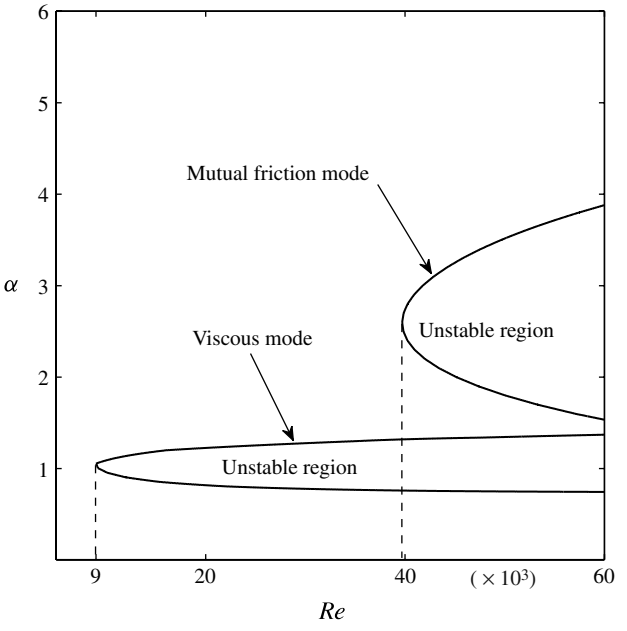

FIGURE 3. Neutral stability curve for the normal fluid with $f_{max} = 0.001$ and $\sigma = 0.15$.

with boundary condition $\tilde{v}_n = \mathrm{D}\tilde{v}_n = \tilde{\eta}_n = 0$ at the walls, using the Chebyshev spectral collocation method (Schmid & Henningson 2001).

3.1. *Modal stability analysis*

In the modal stability analysis we are concerned with the temporal asymptotic behaviour of perturbations. The eigenmodes are considered individually for predicting the stability of the flow. Squire's theorem is valid for parallel flow and the stability analysis is limited to two-dimensional perturbations ($\beta = 0$). A base flow profile is numerically calculated for every Reynolds number (since the similarity profile is absent) and the neutral stability curve is obtained using this varying mean flow profile. A sample neutral stability curve for mutual friction parameters $f_{max} = 0.001$ and $\sigma = 0.15$ is given figure 3.

The neutral stability curve shows two branches representing two modes of instability. The critical Reynolds number for the lower branch occurs for $\alpha = 1.05$ and is similar to classical fluids. Therefore, analogously to classical fluids, this lower-wavenumber mode can be considered as a viscous mode. A second branch of neutral stability curve appears at a higher wavenumber ($\alpha = 2.6$) compared to the viscous mode. This higher-wavenumber mode appears because of the mutual friction term in the normal-fluid governing equation, hence it can be termed the mutual friction mode. The critical Reynolds number due to the viscous mode is higher than in classical fluids, for the particular $f_{max}(=0.001)$ and $\sigma(=0.15)$ values shown in figure 3. Figure 4 shows the variation of growth rate, ω_i, with streamwise wavenumber, α, for the same mutual friction parameters as in the previous figure. The viscous mode alone is unstable at $Re = 10\,000$ and the maximum growth rate occurs for perturbations with $\alpha = 1.05$. The curve for $Re = 50\,000$ shows two regions of positive growth

https://doi.org/10.1017/jfm.2013.35 Published online by Cambridge University Press

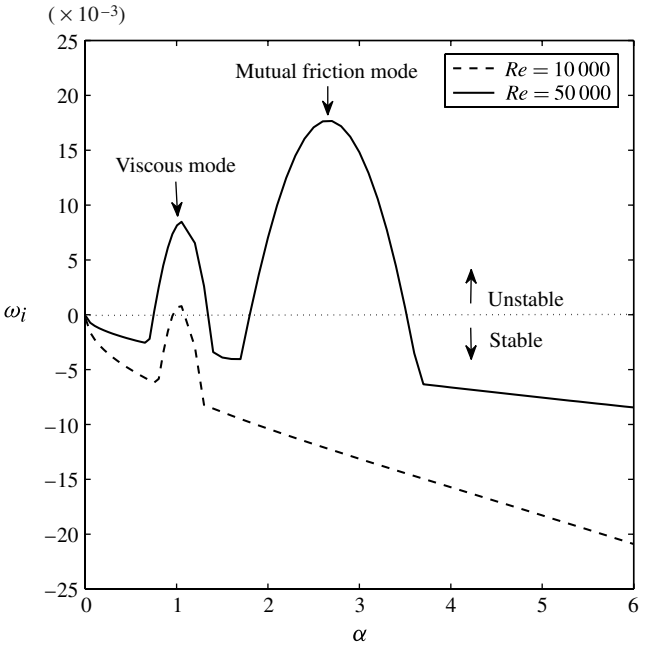

FIGURE 4. Perturbation growth rate, ω_i, versus streamwise wavenumber, α, for Reynolds numbers 10 000 and 50 000. Mutual friction parameters as in figure 3.

rate, corresponding to the viscous mode and the mutual friction mode, at $\alpha = 1.05$ and $\alpha = 2.65$ respectively. The perturbation growth rate is higher for the mutual friction mode, compared to the viscous mode, even though instabilities of the mutual friction mode are triggered only at a higher Reynolds number than the viscous mode. Therefore when Re is high enough, the mutual friction mode is predominant. (The two modes can be viewed as two different mechanisms triggering the instability.) However, these stability characteristics are different when the mutual friction parameters f_{max} and σ are changed, and the two modes becomes less distinct.

Neutral stability curves for different mutual friction parameters are plotted in figure 5. Both the branches, the viscous mode and the mutual friction mode, shift towards lower Re with increase of f_{max}, except at small values of f_{max} where the viscous mode shifts towards higher Re. Thus, the initial nucleation of superfluid vortices stabilizes normal-fluid flow, and any further increase of vortex line density above some critical value starts destabilizing the flow with the appearance of a new mode called the mutual friction mode. At small vortex line densities it is still the viscous mode which has the lower Re_{cr}, but at higher f_{max} mutual friction mode has the lower Re_{cr}. Thus high superfluid vortex line density makes normal fluid more vulnerable to higher-wavenumber instability. The $f_{max} = 0$ curve in the figure is the limiting case, which is equivalent to classical plane Poiseuille flow.

The increase of the σ value causes the neutral stability curve to close, thus forming an island of unstable region. On further increase this unstable region shrinks and at some critical value of σ the unstable region disappears completely, indicating that the normal-fluid flow is completely stable at all Reynolds numbers when σ is greater

https://doi.org/10.1017/jfm.2013.35 Published online by Cambridge University Press

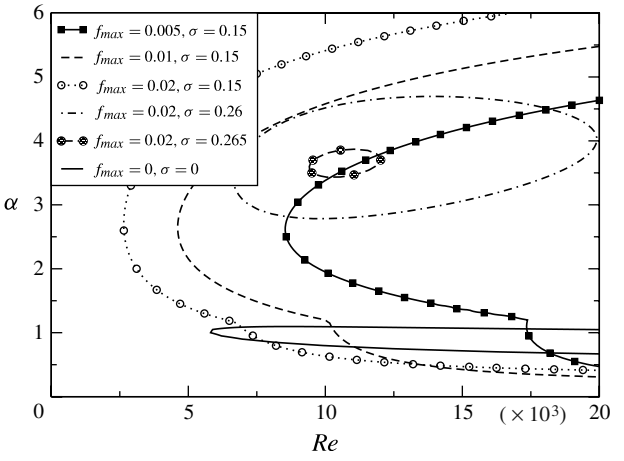

FIGURE 5. Neutral stability curve for the normal fluid with different f_{max} and σ values. Solid line represents classical plane Poiseuille flow neutral curve, which is obtained as the limiting case of $f_{max} = 0$.

than this critical value. Both mechanisms (viscous mode and mutual friction mode) cease to trigger instability in normal fluid above this critical σ value. Thus a uniform distribution of superfluid vortex lines (high σ value) across the channel can completely stabilize the normal-fluid flow. In the limiting case of $\sigma \to \infty$, the function $f(z)$ becomes independent of z.

The variation of critical Reynolds number with σ is shown figure 6. The general pattern in the figure is such that it comprises two parts with different local minima and joined at a point where there is a discontinuity in the slope. The lower-σ region of the curve represents the viscous mode and the higher-σ region represents the mutual friction mode (comparing the α values for Re_{cr} leads to this conclusion). The classical viscous mode has the lower critical Reynolds number for small values of σ whereas the mutual friction mode has the lower critical Re for large σ values. Different curves represent different f_{max} values and each curve is extended only up to certain σ values. This termination of curves represents the shrinking and extinction of closed neutral stability curves.

Figure 7 shows the variation of critical Reynolds number with f_{max}. The two modes are less visible in this graph but the kink at a small f_{max} value represents the separation between the two modes. Similar to figure 6 each curve terminates at a certain critical f_{max} value corresponding to the extinction of the closed loop in the neutral stability curve and beyond this critical value the flow is completely stable. The value of this critical f_{max} varies with σ, and this variation is shown in figure 8. It is observed from the figure that the critical σ, at which flow become completely stable for all Re, is decreasing with increase of f_{max}. The region above the curve is stable for all Re. As mentioned above, high σ means a wider distribution of vortex lines. It may be concluded that it is the vortex line distribution that is important from a stability point of view, rather than the strength of vortex in itself. In short, the local accumulation of superfluid vortex lines may trigger normal-fluid instability. The inset in figure 8 shows the values at large f_{max}, usually found in counter-flow experiments.

https://doi.org/10.1017/jfm.2013.35 Published online by Cambridge University Press

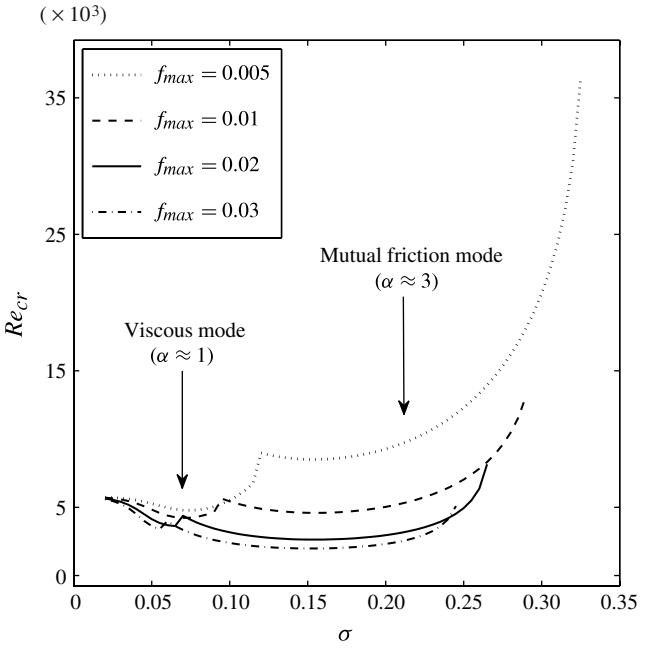

FIGURE 6. Variation of critical Reynolds number with σ for the normal fluid.

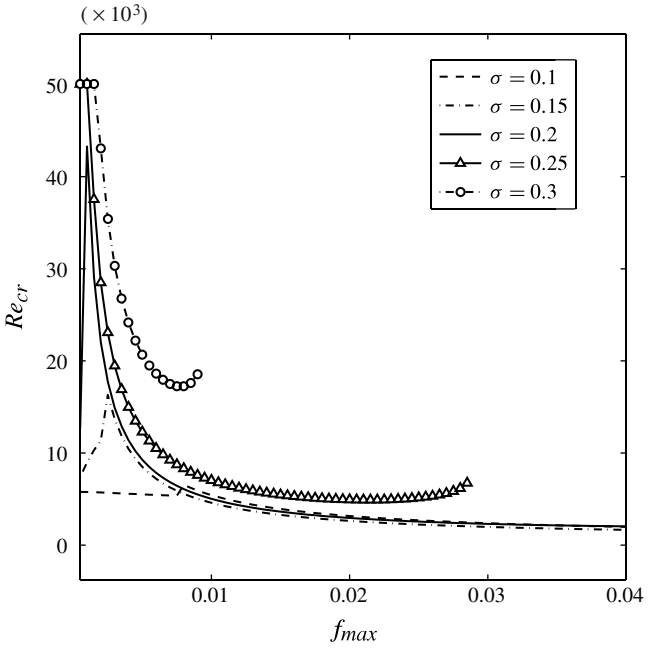

FIGURE 7. Variation of critical Reynolds number with f_{max}.

https://doi.org/10.1017/jfm.2013.35 Published online by Cambridge University Press

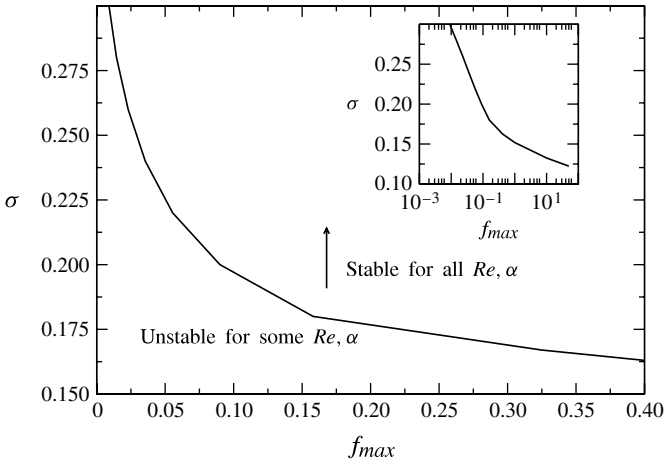

FIGURE 8. Variation of critical superfluid vorticity distribution, σ, with f_{max} at which flow becomes completely stable for all Reynolds numbers. Inset shows the curve extended for large f_{max}. Note that the abscissa is in logarithmic scale.

3.2. *Non-modal stability analysis*

The non-normal nature of the Orr–Sommerfeld and Squire's operators can result in transient growth of the perturbations even when the individual eigenmodes are asymptotically decaying (Schmid & Henningson 2001). In classical plane Poiseuille flow, the transient growth can amplify to the order of 10^2–10^3 which results in subcritical transition to turbulence.

The maximum possible amplification, $G(t)$, of an initial disturbance $\boldsymbol{q}_0$, which is the one optimized over all possible initial conditions, is defined as (Schmid & Henningson 2001)

$$G(t) = \max_{\boldsymbol{q}_0 \neq 0} \frac{\|\boldsymbol{q}(t)\|^2}{\|\boldsymbol{q}_0\|^2}. \tag{3.4}$$

The maximum possible growth function, $G(t)$, is plotted against time in figure 9 for $\alpha = 1$ and $\beta = 0$ and for two different Reynolds number 1000 and 8000 at which classical fluid shows exponentially stable and unstable behaviours respectively. The normal fluid, with parameters $f_{max} = 0.005$ and $\sigma = 0.15$, is exponentially stable at $Re = 1000$. There is a transient growth of perturbations similar to classical fluids but the maximum growth is smaller compared to classical fluids. For $Re = 8000$ and for the same set of wavenumbers as before, where the classical fluid is exponentially unstable, the normal fluid shows a stable behaviour for parameters $f_{max} = 0.01$ and $\sigma = 0.15$ and an unstable behaviour for $f_{max} = 0.03$ and $\sigma = 0.15$. There are two local maxima visible and the maximum of $G(t)$ for normal fluid is seen to occur at a later time than that for classical fluid.

The maximum growth rate function, G_{max}, is defined as the largest possible energy amplification for all times, i.e. $G_{max} = \mathrm{Max}(G(t))$. The contours of G_{max} are plotted in the α–β plane for $Re = 1000$, $f_{max} = 0.03$, $\sigma = 0.15$ in figure 10. The normal fluid with $f_{max} = 0.03$ and $\sigma = 0.15$ has a critical Reynolds number less than the classical plane channel flow; $Re = 1000$ is stable for both flows. However, the non-modal analysis

https://doi.org/10.1017/jfm.2013.35 Published online by Cambridge University Press

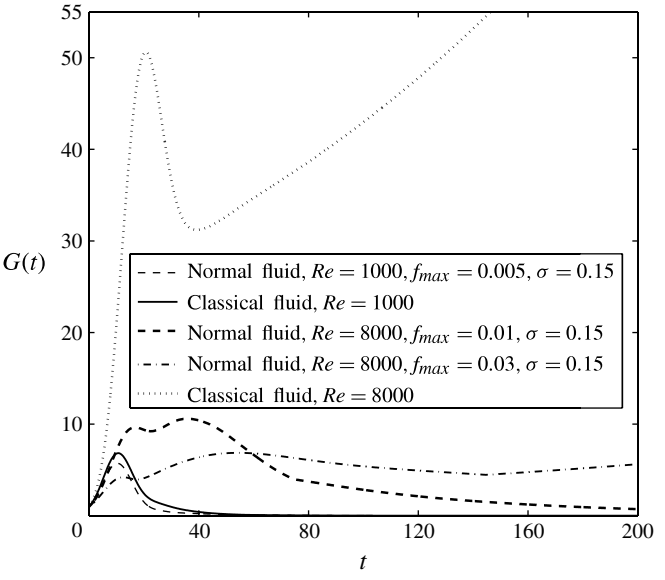

FIGURE 9. Maximum amplification of perturbation, $G(t)$, versus time for normal fluid and classical fluid for two Re values 1000 and 8000 at $\alpha = 1$ and $\beta = 0$.

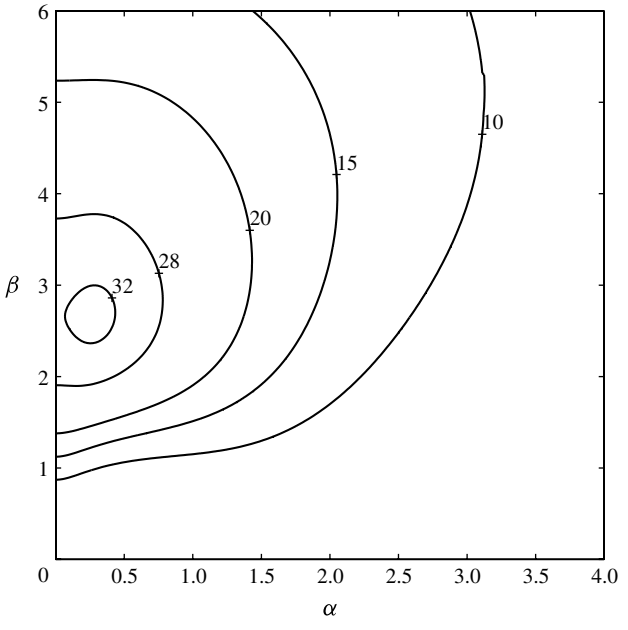

FIGURE 10. G_{max} contours for normal fluid. $Re = 1000, f_{max} = 0.03, \sigma = 0.15$.

https://doi.org/10.1017/jfm.2013.35 Published online by Cambridge University Press

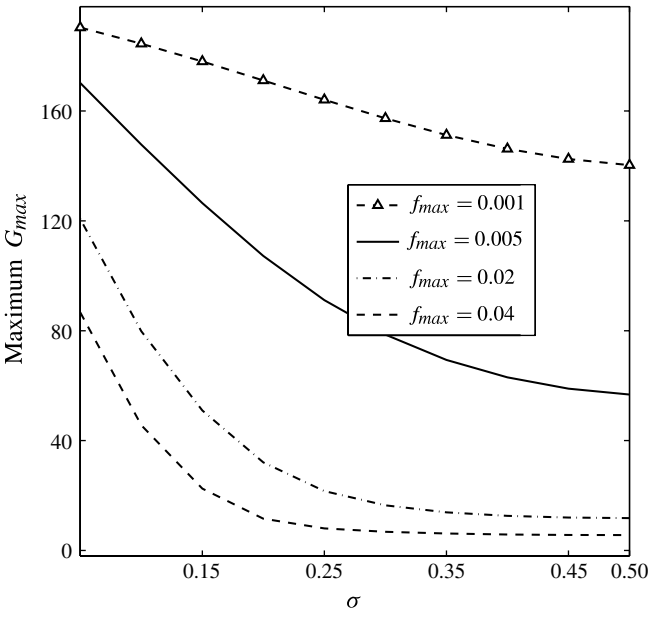

FIGURE 11. Variation of maximum G_{max} with σ for normal fluid at $Re = 1000$.

gives a lower maximum transient growth for the normal fluid than classical fluid. This can be attributed to more flattening of the mean flow profile of the normal fluid, which could also mean that the chance of subcritical instability is less in normal fluid. Unlike classical fluids, the maximum of G_{max} occurs for a non-zero α (streamwise waves), showing that oblique waves have the maximum transient amplification of energy. The above result contradicts the results reported in Bergström (2008) and is attributed to the difference in sign of F_{mf}. The variation of maximum of G_{max} with σ and f_{max} is plotted in figures 11 and 12. The transient energy growth is increasingly less dominant with the increase of σ and f_{max}.

4. Discussion

The mutual friction force was modelled with a bimodal Gaussian distribution for superfluid vortex lines involving parameters f_{max}(peak value) and σ(standard deviation), causing a non-uniform mutual friction forcing. It is easy to show, from equations (1.2)–(1.4), that the parameter f_{max} can be expressed in the following form:

$$f_{max} = \frac{B\rho_s L\kappa l}{\rho V_0}. \tag{4.1}$$

Thus f_{max} can be directly related to superfluid vortex line density, l. In experiments it is the value of l that is measured as the excess attenuation of second sound. By varying the peak value (f_{max}) and spread (σ) of the distribution, one could model different vortex density scenarios, representing different temperatures of superfluid.

The modal analysis showed that both superfluid vortex line density and its distribution have significant effects on the neutral stability. Two modes of instabilities

https://doi.org/10.1017/jfm.2013.35 Published online by Cambridge University Press

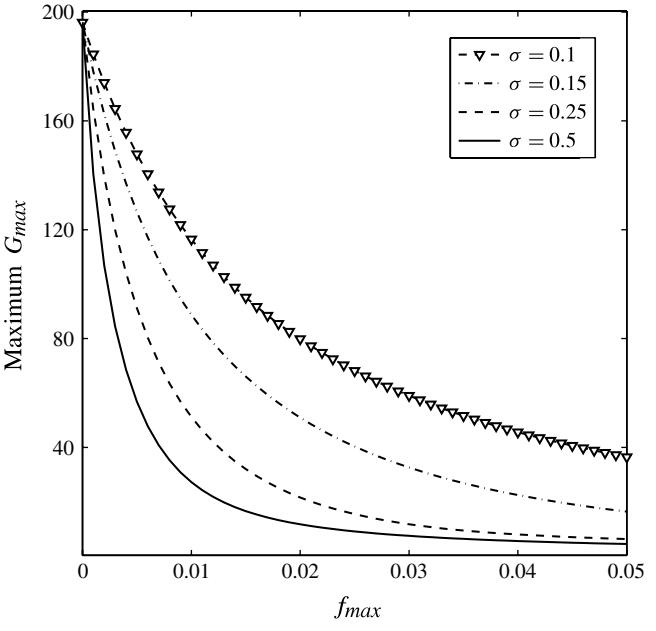

FIGURE 12. Variation of maximum G_{max} with f_{max} for normal fluid at $Re = 1000$.

at different wavenumbers are predicted, which we termed the viscous mode and mutual friction mode. The whole instability region disappeared for every f_{max} when σ exceeded a particular value, indicating a stable regime for any wave at all Reynolds numbers. Thus we consider that a high superfluid vortex line density alone is not enough to induce instability in the normal fluid. A localization of vortex lines can considerably affect the stability. However, the extent of non-uniformity required to cause instability depends on the density itself.

The numerical simulation of superfluid vortex lines by Aarts & de Waele (1994) has shown that they tend to move to points of lower relative velocity between superfluid and normal fluid. Thus it is plausible that increasing Re can make the superfluid vortex line distribution localized or increase its non-uniformity. It is also possible that an increase in Re can increase superfluid vortex line density, due to interaction with the walls and due to the increase of relative velocity of the two fluids. In other words, as Re increases σ decreases and f_{max} increases, thus moving towards the unstable region in figure 8. In the present calculations we have assumed a uniform superfluid velocity profile, and the superfluid vortex line distribution is assumed to be non-uniform across the channel width. In a related recent numerical computation by Galantucci *et al.* (2011) the superfluid velocity profile is shown to be non-uniform. However, they assumed a constant parabolic velocity profile for the normal fluid. In reality as shown in Barenghi (2010) and Guo *et al.* (2010) both profiles may be a function of z and Re. In approximating the mutual friction with (1.3) we have in fact approximated curl of U_s with κl, to represent the vorticity of the superfluid averaged over several quantized vortex lines. If κl is a function of z, U_s is also a function of z, which is inconsistent with our earlier assumption. However, variations in U_s will make only a

https://doi.org/10.1017/jfm.2013.35 Published online by Cambridge University Press

marginal change in the mutual friction (Bergström 2008). More work needs to be done experimentally and theoretically to evaluate both the velocity profiles simultaneously.

In conclusion, the results point to a scenario where the triggering of instability and the subsequent transition in the normal fluid is initiated by a mechanism that is related to mutual friction and makes it distinct from the instability and transition behaviours of classical fluids.

Acknowledgements

We thank Professor C. F. Barenghi for the discussions and his valuable suggestions.

References

AARTS, R. G. K. M. & DE WAELE, A. T. A. M. 1994 Numerical investigation of the flow properties of He II. *Phys. Rev.* B **50**, 10069–10079.

BARENGHI, C. F. 2001 Introduction to superfluid vortices and turbulence. In *Quantized Vortex Dynamics and Superfluid Turbulence* (ed. R. J. Donnelly, C. F. Barenghi & W. F. Vinen). Springer.

BARENGHI, C. F. 2010 Laminar, turbulent or doubly turbulent? *Physics* **3**, 60.

BARENGHI, C. F., DONNELLY, R. J. & VINEN, W. F. 1983 Friction on quantized vortices in Helium II. *J. Low Temp. Phys.* **52**, 189.

BARENGHI, C. F. & JONES, C. A. 1988 The stability of the Couette flow of Helium II. *J. Fluid Mech.* **197**, 551–569.

BERGSTRÖM, L. B. 2008 The initial-value problem for three-dimensional disturbances in plane Poiseuille flow of Helium II. *J. Fluid Mech.* **598**, 227–244.

DONNELLY, R. J. 1991 *Quantized Vortices in Helium II*, 1st edn. Cambridge University Press.

DONNELLY, R. J. & LAMAR, M. M. 1988 Flow and stability of Helium II between concentric cylinders. *J. Fluid Mech.* **186**, 163–198.

DONNELLY, R. J. & SWANSON, C. E. 1986 Quantum turbulence. *J. Fluid Mech.* **173**, 387–429.

GALANTUCCI, L., BARENGHI, C. F., SCIACCA, M., QUADRIO, M. & LUCHINI, P. 2011 Turbulent superfluid profiles in a counterflow channel. *J. Low Temp. Phys.* **162** (3–4), 354–360.

GODFREY, S. P., SAMUELS, D. C. & BARENGHI, C. F. 2001 Linear stability of laminar plane Poiseuille flow of Helium II under a non-uniform mutual friction forcing. *Phys. Fluids* **13** (4), 983.

GUO, W., CAHN, S. B., NIKKEL, J. A., VINEN, W. F. & MCKINSEY, D. N. 2010 Visualization study of counterflow in superfluid ^{4}He using metastable helium molecules. *Phys. Rev. Lett.* **105** (4), 045301.

DE HAAS, W. & VAN BEELEN, H. 1976 A synthesis of flow phenomena in helium II. *Physica* B **83** (2), 129–146.

DE HAAS, W., HARTOOG, A., BEELEN, H. VAN, OUBOTER, R. DE B. & TACONIS, K. W. 1974 Dissipation in the flow of He II. *Physica* **75** (2), 311–319.

HALL, H. E. & VINEN, W. F. 1956*a* The rotation of liquid Helium II. I. Experiments on the propagation of second sound in uniformly rotating Helium II. *Proc. R. Soc. Lond.* A **238** (1213), 204–214.

HALL, H. E. & VINEN, W. F. 1956*b* The rotation of liquid Helium II. II. The theory of mutual friction in uniformly rotating Helium II. *Proc. R. Soc. Lond.* A **238** (1213), 215–234.

LANDAU, L. & LIFSHITZ, E. M. 1959 *Fluid Mechanics*, 1st edn. Pergamon.

MELOTTE, D. J. & BARENGHI, C. F. 1998 Trasition to normal fluid turbulence in Helium II. *Phys. Rev. Lett.* **80**, 4181.

SAMUELS, D. C. 1992 Velocity matching and poiseuille pipe flow of superfluid helium. *Phys. Rev.* B **46**, 11714–11724.

SCHMID, P. J. & HENNINGSON, D. S. 2001 *Stability and Transition in Shear Flows*. Springer.

https://doi.org/10.1017/jfm.2013.35 Published online by Cambridge University Press

SKRBEK, L. & SREENIVASAN, K. R. 2012 Developed quantum turbulence and its decay. *Phys. Fluids* **24**, 011301.

SOORAJ, R & SAMEEN, A 2011 Instabilities in superfluid plane poiseuille flow. *J. Phys.: Conference Series* **318** (9), 092032.

TILLEY, D. R. & TILLEY, J. 2005 *Superfluidity and Superconductivity*, 1st edn. Overseas Press.

TOUGH, J. T. 1982 Superfluid Turbulence. In *Progress in Low Temperature Physics* (ed. D. F. Brewer), vol. 8, Chap. 3, pp. 133–219. Elsevier.

VINEN, W. F. 1957 Mutual friction in a heat current in liquid Helium II. I. Experiments on steady heat currents. *Proc. R. Soc. Lond.* A **240** (1220), 114–127.

VINEN, W. F. 2006 An introduction to quantum tturbulence. *J. Low Temp. Phys.* **145** (1–4), 7.

VINEN, W. F. & NIEMELA, J. J. 2002 Quantum turbulence. *J. Low Temp. Phys.* **128** (5/6), 167.

https://doi.org/10.1017/jfm.2013.35 Published online by Cambridge University Press